URSI AP-RASC, Sydney, Australia, 17 – 22 August 2025

Reconciling super-resolution imaging predictions from the time-reversal cavity and Fourier optics

Elias Le Boudec*(1), Hamidreza Karami(2), Farhad Rachidi(1), Marcos Rubinstein(2), and Felix Vega(3)
(1) Electromagnetic Compatibility Laboratory, EPFL, 1015 Lausanne, Switzerland
(2) Institute for Information and Communication Technologies, University of Applied Sciences and Arts Western Switzerland, 1401 Yverdon-les-Bains, Switzerland
(3) Directed Energy Research Center, Technology Innovation Institute, Yas Island, Abu Dhabi, United Arab Emirates
*elias.leboudec@alumni.epfl.ch

Abstract

The resolution of traditional imaging techniques, including time-reversal imaging, is diffraction-limited. In the theory of the time-reversal cavity, the limit stems from the interference between diverging and converging waves, irrespective of the distance between the direct-time source and the time-reversal mirror. This appears to contradict the well-known fact that evanescent waves in the near field of the source are necessary to obtain subwavelength images. We shed light on this apparent contradiction by drawing explicit links between both approaches. We illustrate the findings with a simulation of a resonant metalens.

1 Introduction

Traditional radio-frequency imaging is known to be diffraction limited, i.e., it is impossible to distinguish details from a source below roughly $\lambda_0/2$, where λ_0 is the illumination wavelength [1]. In Fourier optics [2], this limit is understood to arise from the evanescent nature of waves with high transverse numbers associated with fine (below the wavelength) source details. In time reversal imaging, this same limit appears from the interaction between the converging wave caused by the time-reversal mirror, and the diverging one that exists because of the absence of a time-reversal sink [3]. The latter limit exists irrespective of the shape of the time-reversal mirror; in particular, no matter how close the sensors are to the source. This seems to contradict the well-known fact that the capture of evanescent waves is key to beating the diffraction limit [4].

In this work, we show how to resolve this apparent paradox, which results from a simplistic interpretation of both theories. We illustrate the results in a numerical simulation of a two-dimensional resonant metalens. Doing so, we summarize key properties that a time-reversal subwavelength imaging system must possess.

2 Method

In this section, we review the origin of the diffraction limit in time-reversal and classical optics, highlight the apparent contradiction, propose an explanation to reconcile both approaches, and introduce the simulation setting used to test the explanation.

2.1 An apparent paradox

We begin by recalling the theory of the time-reversal cavity for electromagnetic fields, introduced in [3] and extended in [5]. In this setting, a source radiates electromagnetic fields (the direct-time fields) which are then recorded on a closed time-reversal cavity surrounding the source. These fields are then time-reversed and propagated back from the cavity boundary. Since the source is not present during this backpropagation stage, the time-reversed fields are the sum of a converging and a diverging wave to satisfy the source-free wave equation. In the frequency domain, if the direct-time electric field at an angular frequency $\omega = 2\pi f$ and position $\mathbf{r}$ is denoted by $E_{\mathrm{DT}}(\omega,\mathbf{r})$, then the time-reversed electric field is [3], [5]

$$E_{\mathrm{TR}}(\omega,\mathbf{r}) = E^*_{\mathrm{DT}}(\omega,\mathbf{r}) - E_{\mathrm{DT}^*}(\omega,\mathbf{r}) \tag{1}$$

where $\cdot^*$ denotes complex conjugation. $E^*_{\mathrm{DT}}(\omega,\mathbf{r})$ is a converging wave, equal to the time-reversal of the direct time wave. $E_{\mathrm{DT}^*}(\omega,\mathbf{r})$ is the diverging wave that would be radiated by the time-reversed original source. For an electric dipole, the time-reversed field is proportional to the imaginary part of the electric Green's function, exhibiting a sinc-like behavior at the dipole location. The width of this sinc is determined by the free-space wavenumber k_0, resulting in an approximate focal spot size of $\lambda_0/2$.

In Fourier optics [2], we analyze the fields radiated by a planar source distribution in the xy-plane. The wavenumbers associated with the corresponding Fourier transform are k_x and k_y, and the propagation away from the source occurs in the z direction, associated with the wavenumber k_z. Outside the source region, the propagation obeys a wave equation whose dispersion relation is a sphere in wavenumber space such that

$$k_x^2 + k_y^2 + k_z^2 = k_0^2 \tag{2}$$

Hence, the fields radiate away from the source according to the positive solution

$$k_z = \begin{cases} \sqrt{k_0^2 - k_x^2 - k_y^2}, & k_x^2 + k_y^2 \leq k_0^2 \\ j\sqrt{-k_0^2 + k_x^2 + k_y^2}, & k_x^2 + k_y^2 > k_0^2 \end{cases} \tag{3}$$

where $j^2 = -1$. The propagation involves the delay operator $e^{-jk_z z}$. Hence, small source details, described by high transverse wavenumbers whose norms exceed k_0, have a purely imaginary wavenumber, and the corresponding wave decays exponentially. In other words, details finer than λ_0 are associated with evanescent waves, and far-field sensors must be diffraction-limited. For example [6], the imaging of a rectangular $\ell \times \ell$ aperture in a shield illuminated by a plane wave is a focal spot of surface $\sim \lambda_0^2$ when imaging from the far field. However, at distances less than roughly $\ell/3$, the evanescent wave carries information about the aperture's true size, that is, ℓ^2.

The apparent paradox is that, on the one hand, a consequence of Equation (1) is that the distance between the time-reversal mirror and the source is predicted to have no effect on the focal spot size (i.e., the imaging resolution) and, on the other hand, the source near-field is necessary to obtain subwavelength images (Equation (3)). The nuance needed to solve this apparent paradox is that the Fourier optics approach does not describe how to obtain the image (e.g., through time-reversal, a classical optical lens, a near-field scan, etc.). Indeed, in agreement with the time-reversal theory, time-reversal imaging is always limited to resolutions dictated by Equation (1); however, this limited resolution might exhibit a $\lambda/2$ focal spot much smaller than in a vacuum, as long as $\lambda < \lambda_0$. An academic example is radio-frequency imaging in pure water, with a real part of the electrical permittivity of 80 [7] yielding a $\lambda_0/2/\sqrt{80} \approx \lambda/18$ super-resolution. Additionally, the time-reversal cavity does not provide an explanation of how to improve the imaging resolution (other than the use of a time-reversal sink [8]). There, the classical optical theory comes into play: a path towards super-resolution involves transmitting near-field information to the time-reversal mirror.

In summary, the Fourier optics approach shows that subwavelength information is contained in the source near field. The near-field waves then need to couple to the imaging system, without regard for the distance between the time-reversal mirror and the source region[1].

2.2 Illustration: the resonant metalens

To illustrate the explanation above, we perform a set of two-dimensional radio-frequency simulations. The geometry of the experiments is shown in Figure (1). In the direct-time phase, we measure the scattering parameters from two simultaneous sources (ports 1 and 2) placed either 30 $\%\lambda_0$ or 70 $\%\lambda_0$ apart ($\lambda_0 = 1$ m) to a nine-channel time-reversal mirror indexed from 10 to 18, i.e.,

$$z_{\mathrm{DT}}(f_n) = S_{m,1}(f_n) + S_{m,2}(f_n) \tag{4}$$

$m = 10, \ldots, 18$, over a frequency range f_n from 200 MHz to 320 MHz, every megahertz ($n = 1, \ldots, 121$).

In the time-reversal phase, we measure the scattering parameter from each time-reversal mirror to port 0, placed on the source plane at position x, and vary x from –45 cm to +45 cm in steps of 5 cm, thus obtaining $S_{0,m}(f_n, x)$. We time-reverse the direct-time measurement by taking the complex conjugate of $z_{\mathrm{DT}}(f_n)$. We backpropagate this time-reversed measurement to the image plane ($z = 0$) by multiplying by the scattering parameter $S_{0,m}(f_n, x)$, obtaining the time-reversed field along the x coordinate:

$$z_{\mathrm{TR}}(f_n, x) = \sum_{m=10}^{18} S_{0,m}(f_n, x) z_{\mathrm{DT}}(f_n)^* \tag{5}$$

Finally, we average the frequency dependence out by taking the normalized energy

$$z_{\mathrm{TR}}(x) = \left[\frac{\sum_{f_n} |z_{\mathrm{TR}}(f_n, x)|^2}{\sum_{f_n, m} |S_{0,m}(f_n, x)|^2} \right]^{1/2} \tag{6}$$

The denominator serves as a normalization with respect to the source-to-time-reversal-mirror coupling strength.

Next, we study six imaging cases, illustrated in Figure (1):

(a) Propagation in vacuum, with a far-field time-reversal mirror;

(b) As (a), with a near-field time-reversal mirror;

(c) We introduce a resonant metalens as in [9] with 41 metallic rods of height $\lambda_0/2$ and a pitch of $\lambda_0/40$. First, we place this lens far, i.e., $\lambda_0/2$, from the source, with a far-field time-reversal mirror.

(d) Next, we bring the metalens close ($\lambda_0/20$) to the source.

(e) We bring the time-reversal mirror in the near-field from the source-and-metalens complex, with the metalens far ($\lambda_0/2$) from the source.

(f) Finally, we keep a near-field time-reversal mirror and bring the metalens close ($\lambda_0/20$) to the source.

3 Results

The time-reversed energy $z_{\mathrm{TR}}(x)$ is shown in Figure (2) for a source separation of 30 $\%\lambda_0$ and in Figure (3) for a source separation of 70 $\%\lambda_0$. We show an example of scattering parameter $S_{0,10}(f_n, x = 0\text{ m})$ in Figure (4).

[1] Of course, in practice, the time-reversal mirror is replaced with a finite number of sensors. The placement of these sensors is well known to be critical.

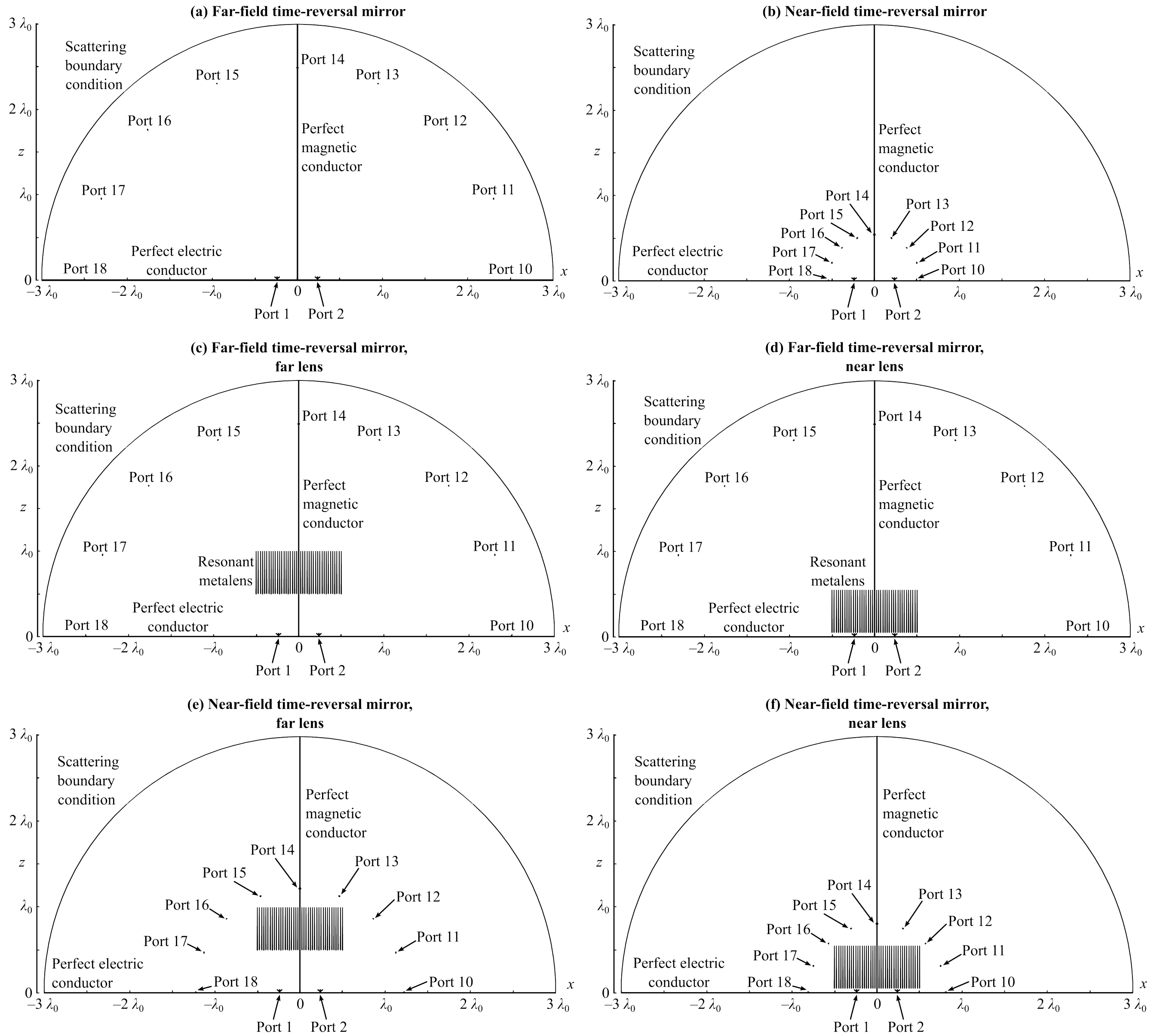

Figure 1. Geometries of all performed simulations.

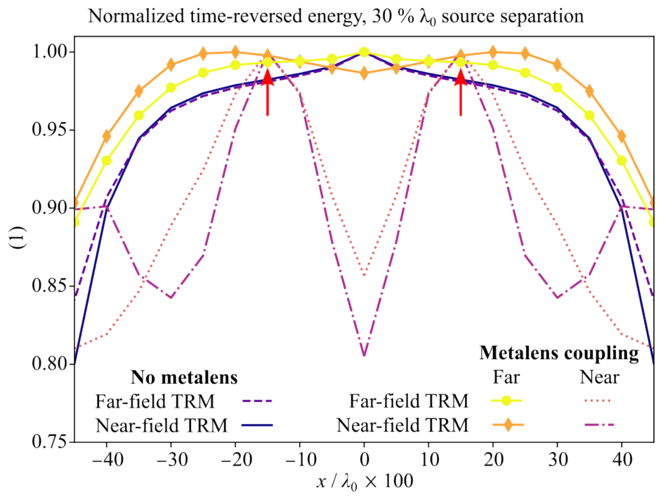

Figure 2. Normalized time-reversed energy $z_{\mathrm{TR}}(x)$ as in Equation (6) for a source separation of 30 $\%\lambda_0$ and the cases shown in Figure (1).

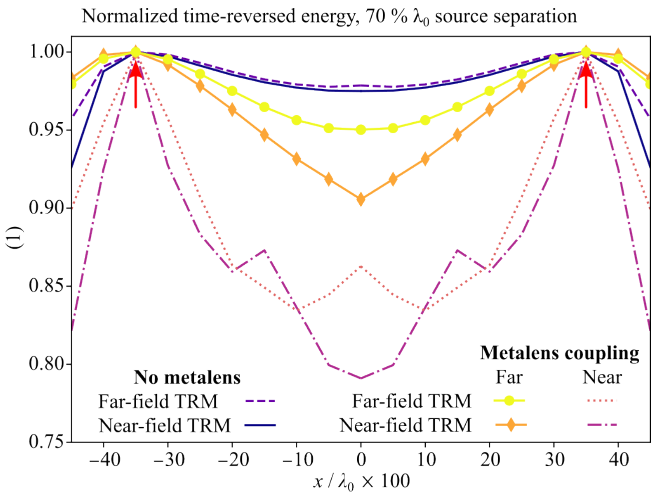

Figure 3. Normalized time-reversed energy $z_{\mathrm{TR}}(x)$ as in Equation (6) for a source separation of 70 $\%\lambda_0$ and the cases shown in Figure (1).

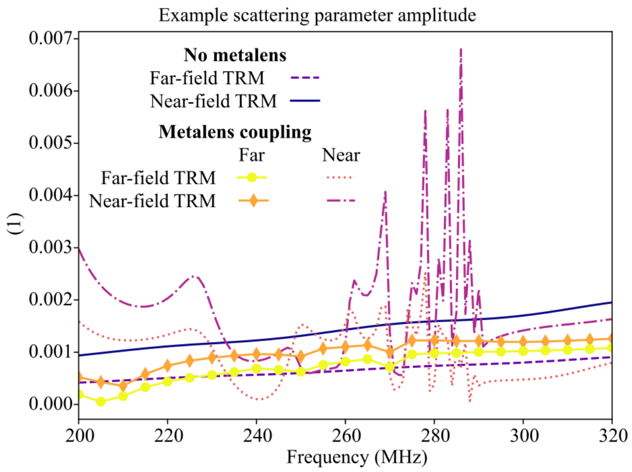

Figure 4. Example time-reversal scattering parameter $S_{0,10}(f_n, x = 0\ \mathrm{m})$ for all cases (a-f) in Figure (1).

4 Discussion

Below the vacuum diffraction limit $\lambda_0/2$, i.e., for a source separation of 30 $\%\lambda_0$, only the metalens placed close to the source can achieve an accurate source localization. Placing the sources further apart (70 $\%\lambda_0$), the sources are distinguishable in all cases, with a clear resolution increase with the resonant metalens.

As expected from the theory of the time-reversal cavity, bringing the time-reversal mirror in the source near-field has a limited effect on the imaging resolution. The small improvement seen in figures (2) and (3) is likely caused by near-field interactions between the metallic parts of the time-reversal mirror and the source and metalens. On the other hand, as expected from the Fourier optics approach, the distance between the source and the metalens is critical to achieve subwavelength imaging: with a distance of $\lambda_0/2$ between the source and the metalens, we see almost no imaging resolution improvement by involving the metalens, even with a time-reversal mirror in the near field.

5 Conclusion

We showed how to solve an apparent contradiction in the theory of super-resolution imaging as observed in the time-reversal cavity and in the Fourier optics perspective. We demonstrated that the distance between the time-reversal mirror and the source has little effect compared to the near-field coupling between the source and a resonant metalens, an important consideration for practical experiments involving metalenses.

Further studies should investigate the link between the obtained resolution and the prediction from the time-reversal cavity for broadband excitation.

References

[1] E. Abbe, "The Relation of Aperture and Power in the Microscope (continued).," *Journal of the Royal Microscopical Society*, vol. 2, no. 4, pp. 460–473, 1882. DOI: 10.1111/j.1365-2818.1882.tb04805.x.

[2] J. W. Goodman, *Introduction to Fourier Optics*, 2nd ed, ser. McGraw-Hill Series in Electrical and Computer Engineering. New York: McGraw-Hill, 1996, 441 pp., ISBN: 978-0-07-024254-8.

[3] R. Carminati, R. Pierrat, J. de Rosny, and M. Fink, "Theory of the time reversal cavity for electromagnetic fields," *Optics Letters*, vol. 32, no. 21, pp. 3107–3109, Nov. 1, 2007. DOI: 10.1364/OL.32.003107.

[4] J. B. Pendry, "Negative Refraction Makes a Perfect Lens," *Physical Review Letters*, vol. 85, no. 18, pp. 3966–3969, Oct. 30, 2000. DOI: 10.1103/PhysRevLett.85.3966.

[5] E. Le Boudec, N. Mora, F. Rachidi, M. Rubinstein, and F. Vega, "Time-reversed electromagnetic fields in anisotropic media," *Optics Letters*, vol. 49, no. 7, pp. 1820–1823, Apr. 1, 2024. DOI: 10.1364/OL.510604.

[6] G. A. Massey, "Microscopy and pattern generation with scanned evanescent waves," *Applied Optics*, vol. 23, no. 5, pp. 658–660, Mar. 1, 1984. DOI: 10.1364/AO.23.000658.

[7] W. J. Ellison, "Permittivity of Pure Water, at Standard Atmospheric Pressure, over the Frequency Range 0–25THz and the Temperature Range 0–100°C," *Journal of Physical and Chemical Reference Data*, vol. 36, no. 1, pp. 1–18, Feb. 8, 2007. DOI: 10.1063/1.2360986.

[8] J. de Rosny and M. Fink, "Overcoming the Diffraction Limit in Wave Physics Using a Time-Reversal Mirror and a Novel Acoustic Sink," *Physical Review Letters*, vol. 89, no. 12, p. 124301, Aug. 30, 2002. DOI: 10.1103/PhysRevLett.89.124301.

[9] F. Lemoult, G. Lerosey, J. de Rosny, and M. Fink, "Resonant Metalenses for Breaking the Diffraction Barrier," *Physical Review Letters*, vol. 104, no. 20, p. 203901, May 18, 2010. DOI: 10.1103/PhysRevLett.104.203901.